EIGHTEENTH EUROPEAN ROTORCRAFT FORUM

B - 21

Paper No. 37

COMPUTATION OF HIGH RESOLUTION UNSTEADY AIRLOADS USING A CONSTANT VORTICITY CONTOUR FREE WAKE MODEL

T. R. QUACKENBUSH
C-M. G. LAM
CONTINUUM DYNAMICS, INC.
PRINCETON, NJ, USA

D. B. BLISS
DUKE UNIVERSITY
DURHAM, NC, USA

September 15-18, 1992

AVIGNON, FRANCE

ASSOCIATION AERONAUTIQUE ET ASTRONAUTIQUE DE FRANCE

COMPUTATION OF HIGH RESOLUTION UNSTEADY AIRLOADS USING A CONSTANT VORTICITY CONTOUR FREE WAKE MODEL

T. R. Quackenbush*, C-M. G. Lam*, and D. B. Bliss**

Continuum Dynamics, Inc.*
Princeton, New Jersey 08543

Duke University**
Durham, North Carolina 27706

Abstract

Recent work in the study of helicopter aerodynamic loading for acoustics applications has involved research on the development of an exceptionally efficient simulation of the velocity field induced by the rotor's vortex wake. This paper summarizes the work to date on the development of this analysis, which builds on the refined Constant Vorticity Contour (CVC) free wake model recently developed for application to the study of vibratory loading. The particular focus of this paper is on demonstrations of a reconstruction approach that efficiently computes both the flow fields and airloads induced by CVC wakes on lifting rotor blades. Results of recent calculations on both main rotor and tail rotors are presented. These calculations show that by employing flow field reconstruction it is possible to apply the CVC wake analysis with temporal and spatial resolution suitable for acoustics applications while reducing the computation time required by one to two orders of magnitude relative to the direct calculations used in traditional methods.

Nomenclature

C_T = rotor thrust coefficient

r_c = physical vortex core radius

r_f = artificial ('fat') vortex core radius

R = main rotor radius

U_∞ = free stream velocity component in X direction

v = vortex swirl velocity

X,Y,Z = global axes centered at the rotor hub

(X positive aft, Z positive down)

α_s = shaft angle of attack

Γ = vortex filament circulation

μ = rotor advance ratio, $U_\infty / \Omega R$

θ = rotor blade root pitch angle

θ_c = HHC amplitude

ψ = azimuth angle of reference rotor blade

Ω = main rotor angular velocity

1. Introduction and Background

The efficient and accurate computation of wake-induced loading on helicopter blades is an important topic for many rotorcraft applications. One such application is rotorcraft noise analysis, where one of the most significant challenges is the problem of prediction of noise from rotor/wake interactions. Such noise is generated both by main rotor / tail rotor interactions and by interactions of main rotor blades with their own wake. Very accurate computation of the wake influence is required for noise calculations, along with high temporal resolution. Previous efforts (Refs. 1 and 2) addressed an important component of the prediction of unsteady loads, namely the analysis of wake-induced flow fields. This work was carried out in part to demonstrate an exceptionally efficient approach to the generation of high-resolution velocity field calculations, based on the method of flow field reconstruction. The work on this topic has covered a wide range of wake/rotor interactions, including the interaction of the main rotor with its own wake (Ref. 1) and main rotor/tail rotor interactions (Ref. 2). The present paper summarizes the work to date on the extension of these methods to the prediction of unsteady aerodynamic loading on rotor blades.

After a brief review of related efforts, some background on the aerodynamic models underlying the present research will be described, in particular the Constant Vorticity Contour (CVC) wake model; examples of its application to unsteady load predictions will also be

described. Then the basic features of the reconstruction methods presently in place will be outlined. Results involving the application of reconstruction techniques to both flow field and airload prediction will be presented, including comparisons to recently acquired measurements of unsteady pressure on tail rotor blades. Finally, plans for the remainder of the present effort will be briefly summarized.

As noted, the motivation for the work described here was the analysis of rotor noise due to wake/rotor interactions. Substantial effort has gone into both experimental and analytical study of the general topic of rotorcraft acoustics in recent years (Refs. 3-8). Experimental studies such as References 3-5 have amply demonstrated the importance of blade/wake interaction in the generation of loading noise. Though recent analytical and computational work has shown some progress toward predicting rotor noise (Refs. 6-8), it is clear that substantial problems remain to be solved.

An obvious prerequisite to successful prediction of rotor noise is accurate analysis of unsteady aerodynamic loading, which in turn depends on an ability to correctly model the structure of the main rotor wake and the velocity field it induces. Recent studies of rotor wake vortex dynamics have produced a rotor wake model that is superior in refinement, consistency, and efficiency to previous treatments. It was found in Reference 9 that in order to successfully predict main rotor aerodynamic loads, it is necessary to account for the vortex wake generated by the entire blade span, not just the tip region. A particularly attractive implementation of a full-span wake involves modeling the wake by a field of constant strength filaments which correspond to the actual resultant vorticity field in the wake (see Fig. 1, which shows the wake of one blade of a four-bladed rotor at advance ratio 0.3). These vortex filaments are laid out on contours of constant vortex sheet strength in the rotor wake, a circumstance that gives the method its name: the Constant Vorticity Contour (CVC) wake model. The CVC wake model treats each curved vortex element as a resultant vector of the local vorticity field, an approach that removes the essentially artificial distinction between "shed" and "trailed" vorticity. Figure 1 shows the very complicated incident wake structure generated by typical rotors; this complex structure leads to a wide range of possible interactions of the wake with the main rotor blades, as well as significant main rotor/tail rotor (MR/TR) interactions.

2. Correlation Studies Using the CVC Wake Model

References 10 and 11 discuss the development of the CVC vortex dynamics analysis method and document its success in the prediction of main rotor blade unsteady airloading. The resulting code, denoted RotorCRAFT (Computation of Rotor Aerodynamics in Forward flighT), uses a vortex lattice representation of the blade to predict aerodynamic loads and a finite element model of the rotor blade structure. RotorCRAFT incorporates a full flap/lag/torsion aeroelastic model that captures realistic blade deflections, as well as a trim algorithm that ensures that rotor loading is calculated for realistic load distributions. References 10 and 11 describe the application of RotorCRAFT to a variety of calculations of practical importance, including studies of steady and unsteady aerodynamic loads on rotors in both high- and low-speed flight.

Reference 12 describes the extension of these airload prediction methods to computation of blade stresses and hub loads. This work was motivated by the desire to support recent research into the application of higher harmonic pitch control to the alleviation of rotor noise (Ref. 13). Experimental studies have shown considerable promise in the strategy of applying four-per-rev(4P) root pitch control to reduce rotor noise. However, the effect of such control strategies on vibratory load levels must be considered. To address such issues, an extended version of RotorCRAFT was developed that allowed for the calculation of internal blade stresses as well as forces and moments at the rotor hub.

In Reference 13, tests conducted on a four-bladed model rotor in the Transonic Dynamics Tunnel (TDT) at NASA/Langley are described. The rotor was untwisted and untapered and had a radius of 4.58 ft. and a chord of 0.35 ft.; the rotor was operated at a thrust coefficient of 0.005 and a tip Mach number of 0.62. The tests included a range of flight conditions and shaft angles of attack to simulate rotors in both level and descending flight.

Ref. 12 focused on four of these flight conditions: $\mu = 0.166$, $\alpha_s = 4.0$ deg. (Case A), $\mu = 0.3$, $\alpha_s = 2.0$ deg (Case C), $\mu = 0.166$, $\alpha_s = 0.0$ deg (Case G), and $\mu = 0.3$, $\alpha_s = -4.0$ deg (Case I). Figure 2 shows the correlation obtained using RotorCRAFT to predict the magnitude of the measured 4P hub loads for cases without higher harmonic pitch inputs. The agreement is very good over the range of cases examined. Reference 13 also describes the application of higher harmonic root pitch of various magnitudes and phase angles to reduce rotor noise. RotorCRAFT can take as input arbitrary periodic pitch time histories including higher harmonic forms such as :

$$\theta(\psi) = \theta_0 + \theta_{1c}\cos\psi + \theta_{1s}\sin\psi + \ldots + \theta_{nc}\cos n\psi + \theta_{ns}\sin n\psi + \ldots$$

For these correlation calculations, the steady and first harmonic pitch inputs were chosen to trim the rotor to zero first harmonic flapping at the desired thrust coefficient of 0.005. All other harmonic components were set to zero, except the 4P terms. Reference 13 specified the 4P inputs in terms of a magnitude θ_c and a phase angle ψ_c, such that $\theta_{4c} = \theta_c\cos 4\psi_c$ and $\theta_{4s} = \theta_c\sin 4\psi_c$. Sample results of the correlations carried out for the pitch amplitude $\theta_c = -0.6°$ are shown in Figure 3. These indicate that generally good correlation of the 4P hub force magnitude was obtained for the operating conditions considered. These results, in addition to those generated as a result of previous work, have provided encouraging evidence of the physical fidelity of the CVC wake model in the RotorCRAFT code.

3. Flow Field and Airload Reconstruction

These results address the prediction of unsteady loads that contribute to rotor vibration, but aerodynamic loads of much higher frequency must be resolved to predict rotor noise. This means that very small time steps must be used to discretize each rotor revolution. Since the CVC wake model is a Lagrangian description of the vortex wake, it suffers from the problems with computational efficiency common to all such methods when very high temporal resolution of the flow is required. A so-called 'reconstruction' approach has been developed to allow the refined flow field model inherent in the CVC wake description to be retained while reducing the computational requirements from one to two orders of magnitude relative to direct, conventional Lagrangian computations of unsteady vorticity fields.

The first step in motivating the reconstruction approach is to appreciate that the rapid temporal variations in the velocity field (and airloads) observed on rotor blades encountering the vortex wake are directly related to the steep spatial velocity gradients they experience during such interactions. Small time steps are required to resolve these interactions, leading to large CPU times for conventional Lagrangian models. Now consider a different approach that could circumvent this problem. First assume that the core size of the main rotor vortices penetrating or approaching a region of interest could be increased arbitrarily (the "region of interest" or "evaluation region" is typically a grid of points on the main rotor or tail rotor blades). This would make the velocity gradients encountered by the rotor blades much smoother and, consequently, far fewer time steps would be required to resolve the blade loads to an acceptable degree of accuracy. A simulation with artificially "fat" vortex cores could thus be undertaken with the full-span CVC wake using reasonable amounts of CPU time, but the solution would be physically meaningless because of the artificial smoothing. However, if the use of the fat core were restricted to computation of the induced velocity in the region of interest and the actual vortex core were used elsewhere (e.g., wake-on-wake interactions) then the motion of the vortex wake through the region of interest would be correct; any errors due to the use of the fat core would only affect the nearfield flow used to compute wake-induced velocities .

This approach assumes that the correct velocity profile inside the vortex core (i.e., the 'actual core' solution) is known or that the analyst is willing to specify a suitable approximation to it. Given this additional assumption, it is possible to construct nearfield corrections to recover the physically correct solution with the actual core. Since this correction scheme is applied only to the relatively small number of points of evaluation in the region of interest, the total CPU time required should be negligible compared to the CVC rotor wake calculation

required to define the wake geometry. Using this general approach, then, computations yielding high spatial and temporal resolution of the wake flow field could become much more efficient, since high local accuracy is obtained by matching in an appropriate nearfield solution rather than by direct computation of the vortex wake geometry using small time steps. Clearly, the execution of such a local nearfield correction is crucial to the accuracy of this method, and a further discussion of the nearfield correction scheme used here is given in Refs. 1 and 2; a brief summary is given in later in this section.

This correction scheme is an important part of the complete reconstruction process, which can be summarized as follows. First, the CVC free wake model in RotorCRAFT is run for a specified number of main rotor revolutions using relatively coarse time steps, usually between twenty and forty steps per main rotor revolution. At each time step the velocity field generated at specified points within a user-defined evaluation region is calculated and stored. Simultaneously, the positions and orientations of vortex filament intersections with a reference plane (referred to as a "scan plane" for present purposes) are also recorded. The scan plane(s) typically intersect the evaluation region in one or more directions (Fig. 4); the role of the scan plane is to define a convenient reference for the nearfield correction terms to be applied, as will be discussed below. These computations comprise the initial (and by far the most computationally costly) phase of the overall analysis. It is important to note that this calculation requires vastly less computation time than would a direct calculation at the refined time steps normally required for acoustics calculations.

Once this portion of the simulation is completed, a reconstruction program is used to take the stored information on the wake-induced velocity field and the "tracks" of the vortex intersections with the scan planes and regenerate the velocity field induced by the transit of the actual wake vortices through the region of interest. This is accomplished by first interpolating the smoothed velocity field generated by using the fat core to yield the "background" flow at each of the evaluation points, i.e. a low-resolution solution for the flow field. Note that this is interpolation in time, which can be carried out in confidence because the use of the fat core has eliminated the steep velocity gradients from the velocity field at the points of evaluation. Second, the positions of the vortex intersections with the scan planes are also interpolated provide the information needed for producing high temporal resolution flow histories. By applying the nearfield analytical correction terms detailed in References 1 and 2 to the low-resolution flow computed using the fat core, the velocity induced using the actual vortex core can be recaptured while simultaneously refining the time history of the flow field at the evaluation points. The reduction in CPU typically scales with the cube of the temporal interpolation factor, i.e., an interpolation factor of 5 should yield roughly two orders of magnitude reduction in CPU time. A flow chart depicting the major features of the analysis is given in Figure 5. Note that this flow chart depicts the generation of aerodynamic loads as well as high resolution flow field calculations; the methods used for the computation of such loads will be outlined in the next section.

The reconstruction procedure described above is complex to implement, but once in place it yields not only dramatic reductions in CPU time but also high degree of flexibility and robustness. Previous methods using approaches superficially similar to that described here have in fact been based on ad hoc treatment of close interaction effects. One of the strengths of the present implementation is that the nearfield velocity corrections are produced by a formal matching procedure similar to the method of matched asymptotic expansions. This method is one application of the technique known as Analytical/Numerical Matching (ANM), an approach to problems in vortex dynamics described in several recent papers (Refs. 14-16). This remaining discussion in this section briefly summarizes the application of ANM in this context.

As noted above, the numerical free wake velocity field first is smoothed with an artificially fat vortex core when velocities at the evaluation points in the evaluation region are computed. Because this smoothing produces very gradual variations in velocity, only relatively few calculation points are required to reconstruct this velocity field accurately in the designated region of interest. The fat core smoothing is used only to calculate wake effects at the evaluation points, whereas the actual core is used when calculating velocities on the wake itself. This means that the vortex filament motions are still being accurately computed. Given the geometry and trajectory of the filaments, an analytical solution is then developed based on

the nearfield filament configuration. This solution incorporates the local position and curvature of the filament modeled as a parabolic arc. Actually, to compute the correction term that removes the error introduced by using the fat core, two such analytical solutions are superimposed. One solution adds the contribution of a vortex filament with a physically realistic core, and the other solution subtracts a vortex filament with the same fat core used in the numerical calculation. The net effect in the near field is to cancel the numerical fat core effect and add the effect of the actual core size. At the same time, the far field effect remains unchanged since the two portions of the analytical solution cancel in the far field. The superposition of analytical and numerical solutions is shown in Figure 6.

Typically, "fat" vortex cores used here were three to four times the size of the baseline "actual" core. The numerical smoothing is achieved by use of a particular vortex core model chosen for its ease of implementation, smooth behavior, and its functional simplicity. In its two-dimensional form, the vortex swirl velocity is expressed as $v = (\Gamma/2\pi)r\,(r^2 + r_c^2)^{-1}$. For small r ($<< r_c$) the velocity behaves as if in solid body rotation, whereas for large r ($>> r_c$) the velocity behaves as an irrotational point vortex. When velocities are computed in the evaluation region, r_c is replaced by r_f, where r_f is a fat core radius to provide smoothing; for all other velocity calculations a physically realistic value of core radius r_c is used. It is important to note that this choice of a vortex core model was not intended as an accurate description of the core flow field, but rather as a representative model suitable for use in an interim analysis. The "actual" vortex core sizes were chosen to be typical of those visualized or inferred from flow field data in the literature. One of the strengths of the reconstruction approach implemented here is that the nearfield solution can take nearly any analytical form. Even relatively complex local flow fields representing, for example, decayed ("old") or turbulent core structures may be built into the nearfield solution without impairing the computational efficiency of the method.

4. Example Problems in Flow Field and Airload Reconstruction

To demonstrate the capabilities of the reconstruction analysis, several sample calculations have been undertaken.

4.1 Flow Field Reconstruction

The rotor chosen for the first of these sample calculations is the H-34 main rotor, a four-bladed design with linearly twisted, constant-chord blades. The operating condition selected is advance ratio 0.39 and a thrust coefficient of 0.0037. This rotor was selected because it was closely studied during a previous research effort and its properties and operating characteristics are well understood. As is shown in References 10 and 11, good correlation has been achieved with experimental data on H-34 aerodynamic loading. Though there is no direct measure of unsteady flow fields available for this rotor, it was judged that a close correlation of airloads was a suitable indirect measure of good reproduction of the physical flow field.

The first calculation involved a fixed grid of evaluation points in the vicinity of the advancing tip of the H-34. The case considered here involved a shaft angle of attack of 5 degrees. This flight condition causes the rotor wake to come up through the rotor disk and produce significant blade/wake interactions. The point selected for the H-34 case corresponded to the location of the advancing tip at $\psi = 90$ deg., i.e. $X = 0$, $Y = R$. At this point, a fixed observer should see a rapidly varying upflow and downflow due to the wake of the passing blade (Note: the velocity field of the bound circulation on the blade is not included in these calculations). This behavior is indeed reflected in the result for the original flow field calculation using the assumed actual core size of 0.02R for the baseline calculation and 64 time steps per azimuth (see Fig. 7). The low-resolution fat core solution obtained using a core size multiplier of 3.0 is also shown in Figure 7a; this calculation used 16 time steps per revolution. Finally, the reconstructed curve in the figure represents the result of 4:1 time interpolation of the fat core result, as well as application of the nearfield corrections. (Note that all of the results are normalized by the momentum theory value for uniform downwash at these forward speeds). As is evident, the accuracy of the reconstruction is very good. The complete process of running the initial low-resolution solution and applying the nearfield corrections required

less than 2% of the CPU time used by the direct free wake calculation with the conventional Lagrangian analysis.

The fixed grid results were extended to moving grid calculations using scan planes that rotate with the rotor blade, as shown in Figure 4 shows a typical scan plane orientation for moving grid calculations, with the crossing point being located at 0.9R. The points of velocity evaluation were positioned on the blade surface as it moved around the azimuth. The first reconstructed result used a point of evaluation at r/R=0.9 on one of the H-34 blades. This run was again done with 4:1 time interpolation, and this yielded the comparison given in Figure 7b. The reconstruction is very good, increasing confidence that flow field data can be accurately reconstructed to the desired level of time resolution for acoustics calculations. Some sensitivity remains to the exact location of the scan planes used in to capture all possible interactions, as is discussed in Reference 1. Systematic study of the optimum location of scan planes is part of ongoing work in this area.

4.2 Surface Pressures

The primary long-term applications of this work the prediction of the noise due to rotor blades interacting with wake vortices. The intermediate step between the flow field calculation and the computation of noise is the determination of the blade surface pressures, for use in analyses like WOPWOP (Ref. 17). An important part of recent work has been the extension of flow field reconstruction to surface pressures. Work to date has included correlation studies with surface pressure measurements on a tail rotor taken in flight (Refs. 18,19).

It was judged appropriate for the present effort to adopt a relatively simple model based on the selection of an aerodynamic transfer function to predict the lift response to the unsteady upwash field experienced by the rotor blades. In the present calculations, the upwash on each of rotor blades is modeled as an arbitrary gust. A modified Wagner function is used in conjunction with a novel method for the computation of near wake induced velocity response to this arbitrary gust. This treatment is tailored to smoothly merge the 3D vortex lattice analysis used to represent the rotor blades and the CVC filamentary wake. The analysis includes both the effect of the time-varying free stream and the unsteady wake-induced upwash. Both the amplitude of the pressure response and the nondimensional time in this analysis are adjusted for compressibility using a correction in the spirit of Prandtl-Glauert.

The actual surface pressure calculation for a given sectional lift was estimated using off-line calculations with a three-dimensional panel method for thick lifting surfaces modeled on a widely used industrial code (Ref. 20). For the purposes of the present calculations, each section of the rotor blade was considered locally two-dimensional and a single relationship between lift coefficient and surface pressure was developed. This simplifying assumption means that errors will be introduced in a region a few blade thicknesses wide near the blade tip. This approximation was considered acceptable for the purpose of carrying out the preliminary correlation studies described here.

The data for this correlation is drawn from recent experimental studies of tail rotor loading at the Royal Aerospace Establishment. This work has involved the acquisition of a unique body of data on the unsteady surface pressure on tail rotor blades in the presence of the main rotor wake (Ref. 18,19). The data was taken on one blade of the tail rotor of an Aerospatiale Puma in flight in hover and 10, 20, and 30 knots in forward flight. The tests measured the instantaneous pressure coefficient at 2% chord; this local value of C_p has been found to be a suitable indicator of the sectional lift coefficient. With the assistance of RAE personnel, data has been obtained containing the unsteady pressure measurements for the 30 knot case.

Figure 8 shows a representative plot of the pressure data discussed in Ref. 19; this figure is a polar contour plot which represents a complete time history of the pressure coefficient at 2% chord for a full rotor rotation. It is important to note that this does not represent an instantaneous "snapshot" of pressure over the disk but rather a continuous sweep of a single blade over the disk, representing a complete tail rotor period. Because the tail rotor rotation frequency is not an integral multiple of the main rotor frequency, these plots repeat themselves

only over very large numbers of tail rotor periods; thus, time domain simulations must be carefully phased with the position of the generating blade on the main rotor. Also, the time increments in the measurements correspond to roughly 100 steps per tail rotor revolution, so a high temporal interpolation factor must be used to obtain appropriate resolution.

A calculation was carried out to explore the application of reconstruction to the prediction of surface pressures on the instrumented tail rotor in the presence of the main rotor wake. The Puma main rotor has four blades of radius 26.7 ft. and a constant chord of 1.98 ft. The advance ratio for this case was 0.072, and the main rotor thrust coefficient was assumed to be 0.0059. (Flight test data and geometric layout information supplied by RAE allowed the trim condition of the aircraft to be estimated). The computational model of the main rotor wake used four turns of free vortex wake; a baseline calculation was carried out involving forty time steps per main rotor revolution, corresponding to roughly eight time steps per tail rotor revolution, given the 4.82:1 gear ratio. To obtain reasonable reconstruction of the tail rotor loading, at least 40 time steps per tail rotor revolution are required, thus requiring roughly 5:1 time interpolation factor in the reconstruction. The reconstruction procedure (Fig. 5) was used to yield a high resolution description of the inflow induced by the main rotor wake on the tail rotor. This reconstruction calculation was carried out using 5:1 time interpolation and a fat core multiplier of 3.0. This led to a reduction in CPU of over a factor of 100 relative to a direct calculation of the velocity field at the tail rotor disk.

Figure 10 shows the results of a computation carried out using reconstruction of the main rotor inflow but assuming two different inflow models for the tail rotor's own wake. The first (Figure 10a) uses an efficient but approximate downwash model based on a simple skewed helix model of the vortex wake (Ref. 21); this model fails to capture major elements of the structure of the pressure loading in Figure 9. A second calculation was undertaken using a freely distorting model of the tail rotor wake. This calculation produces superior results, capturing many of the major qualitative and quantitative features of the measured loading and indicating the importance of the tail rotor's own wake in this case. Of course, the use of a free vortex wake model for both the tail rotor and the main rotor exacts a computational penalty, but this may be alleviated by applying reconstruction to the tail rotor flow field calculation itself before proceeding with the computation of airloads. Also, the present calculation has only a relatively coarse vortex lattice on the tail rotor blade (40 spanwise by 1 chordwise). This, combined with the tail rotor time step presently in use (40 per TR rev), is not sufficient to capture some of the main rotor vortex interaction events. Calculations with higher chordwise load resolution and higher time interpolation ratios (i.e., smaller time steps in the reconstruction) are currently underway.

5. Summary and Future Work

Work to date on this effort has primarily been directed toward demonstrating the feasibility of applying reconstruction techniques using the CVC wake model to the prediction of high resolution airloads. The reconstruction approach permits such calculations to be carried out with dramatically reduced computation time compared to conventional methods. The original formulation and implementation of flow field reconstruction for main rotors and tail rotors has been extended to directly address the loads induced by wake/rotor interactions. Demonstration calculations have been carried out on realistic rotor configurations in both high- and low-speed flight and have shown that the current reconstruction procedure can produce high resolution predictions of the wake-induced flow field with a reduction of from one to two orders of magnitude in CPU, with no sacrifice in the refinement of the wake model or in the accuracy of the prediction. In addition, the application of reconstruction to the computation of tail rotor surface pressures has yielded promising predictions of tail rotor loading as measured in flight, again with large reductions in CPU relative to direct calculations. However, research on the application of reconstruction to the calculation of high resolution unsteady airloads for acoustics applications is ongoing. Important topics in the near term will include: exploring tail rotor surface pressure calculations with enhanced temporal and spatial resolution; developing refined models of the vortex core, to capture realistic swirl velocity distributions; improving the treatment of surface pressure calculations using 3D, compressible, unsteady surface singularity models; further accelerating ree wake calculations through the application of fast vortex methods recently developed for application to interactional aerodynamics; and, finally,

more extensive data correlation efforts on both aerodynamic loads and rotor noise calculations, using NASA's WOPWOP code.

Acknowledgements

The assistance of Lt. A.D.S. Ellin of the Royal Aerospace Establishment in providing the Puma tail rotor data used herein is gratefully acknowledged. This research was sponsored by NASA/Langley Research Center under contract NAS1-19023. The Technical Monitor was Dr. Thomas Brooks.

References

1. Quackenbush, T.R., et al.: "General Flow Field Analysis Methods for Helicopter Rotor Aeroacoustics", AIAA Paper 91-0591, Jan. 1991.
2. Quackenbush, T.R. and Bliss, D.B.: "High Resolution Flow Field Predictions for Tail Rotor Aeroacoustics", AIAA Journal, Vol. 28, No. 11, Nov. 1991.
3. Jacobs, E.W. and Shenoy, R.K.: "Acoustic Characteristics of Tail Rotors of the Effects of Empennage Interactions," Proc. of the 43rd Annual Forum of the AHS, May 1987.
4. Edwards, B.D., Peryea, M.A. and Brieger, J.T.: "1/5th Scale Model Studies of Main Rotor and Tail Rotor Interactions," Proc. of the AHS National Specialists' Meeting on Aerodynamics and Aeroacoustics, Feb. 1987.
5. Liu, S.R. and Marcolini, M.A.: "The Acoustic Results of a United Technologies Scale Model Helicopter Rotor Tested at DNW", Proc. of the 46th Annual Forum of the AHS, May 1990.
6. Marcolini, M., et al.: "Prediction of BVI Noise Patterns and Correlation with Wake Interaction Locations", Proc. of the 48th Annual Forum of the AHS, June 1992.
7. Ziegenbein, P.R.: "The Development of a Prediction Method for Blade-Vortex Interaction Noise Based on Measured Airloads", Proc. of the AHS/RAeS Specialists' Meeting on Rotorcraft Acoustics, Philadelphia, PA, Oct. 1991.
8. Visintainer, J., et al.: "Acoustic Predictions Using Measured Pressures from a Model Rotor in the DNW", Proc. of the 47th Annual Forum of the AHS, May 1991.
9. Bliss, D.B., Dadone, L.U. and Wachspress, D.A.: "Rotor Wake Modeling for High Speed Applications," Proc. of the 43rd Annual Forum of the AHS, May 1987.
10. Quackenbush, T.R., et al.: "Computation of Rotor Aerodynamic Loads in Forward Flight Using a Full Span Free Wake Analysis", Continuum Dynamics, Inc., Report No. 90-05, final report to NASA under contract NAS2-12838, Dec. 1990.
11. Quackenbush, T.R., et al.: "Computation of Rotor Aerodynamic Loads in Forward Flight Using a Full-Span Free Wake Analysis," AIAA Paper 91-3229, Sept. 1991.
12. Quackenbush, T.R., et al.: "Analysis of Rotor Vibratory Loads Using Higher Harmonic Pitch Control," NASA CR 189591, Apr. 1992.
13. Brooks, T. and Booth, E.: "Rotor Blade/Vortex Interaction Noise Reduction and Vibration Using Higher Harmonic Control", Proc. of the 16th European Rotorcraft Forum, Sept. 1990.
14. Quackenbush, T.R., and Bliss, D.B.: "Free Wake Flow Field Calculations for Rotorcraft Interactional Aerodynamics", Vertica, Vol. 14, No. 3, 1990.
15. Bliss, D.B. and Miller, W.O. : "Vortex Filament Calculations by Analytical/Numerical Matching with Comparisons to Other Methods", AIAA Paper 89-1962, June 1989.
16. Miller, W.O. and Bliss, D.B.: "Direct Periodic Solutions of Rotor Free Wake Calculations by Inversion of a Linear Periodic System", Proc. of the 46th Annual Forum of the AHS, May 1990.
17. Brentner, K.S.: "Prediction of the Helicopter Rotor Discrete Frequency Noise," NASA TM 87721, Oct. 1986.
18. Ellin, A.D.S.: "Flight Measurements Illustrating Key Features of Tail Rotor Loading Distribution", presented at RAE Conference on Yaw Control, London, U.K., Feb. 1990.
19. Ellin , A.D.S.: "Tail Rotor Aerodynamic Features Recorded in Flight", Proc. of the Sixteenth Annual European Rotorcraft Forum, Glasgow, Scotland, Sept. 1990.
20. Magnus, A.E., and Epton, M.A.: "PANAIR Theory Document", NASA CR 3251, Nov. 1981.
21. Coleman, R.P., et al.: "Evaluation of the Induced-velocity Field of an Idealized Helicopter Rotor", NACA ARRL 5E10, 1945.

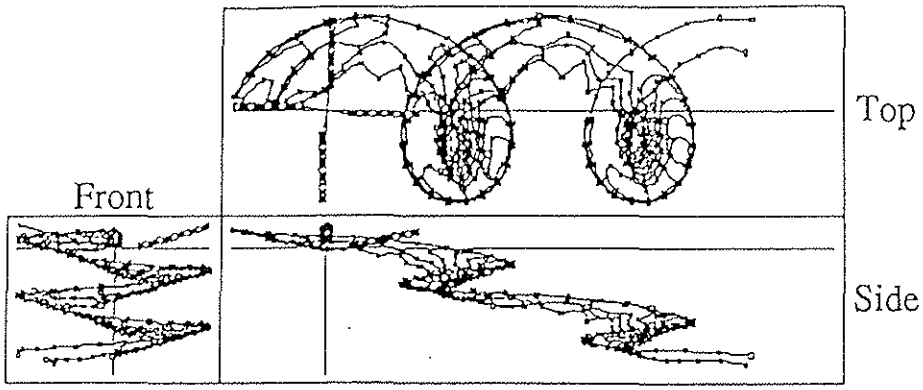

Figure 1. Wake geometry for one blade of a four-bladed rotor at advance ratio 0.3 using the Constant Vorticity Contour (CVC) wake model. (Only two turns of the full-span CVC wake are shown; vertical scale expanded by a factor of 5.0 .)

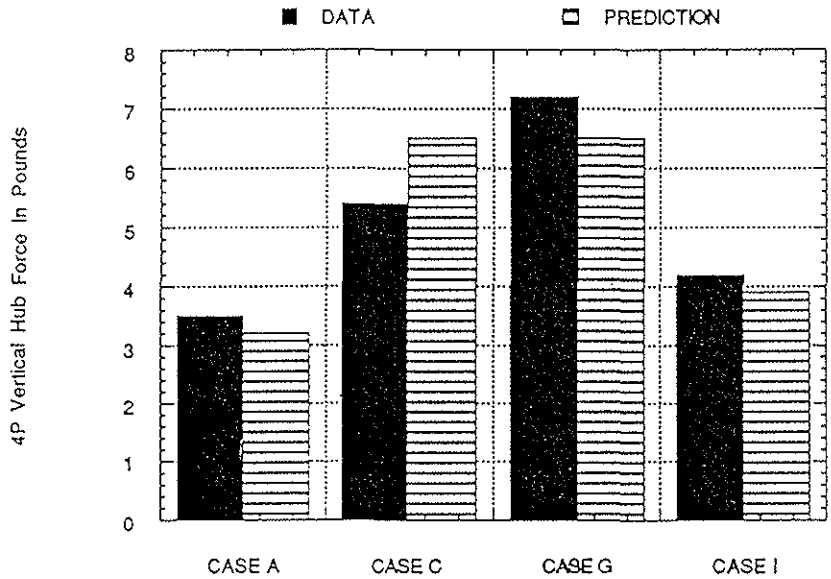

Figure 2. Comparison of predicted and experimental 4P vertical (hub) force amplitude using the RotorCRAFT code. CASE A (μ=0.166, α_S=6.0°), CASE C (μ=0.300, α_S=2.0°), CASE G (μ=0.166, α_S=0.0°), CASE I (μ=0.300, α_S=-4.0°).

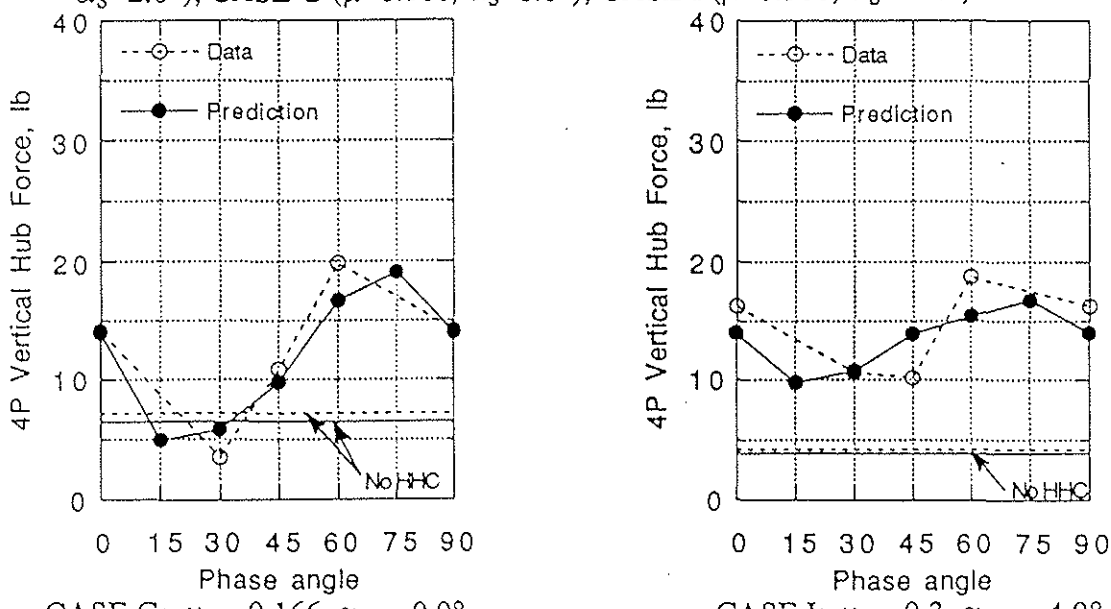

CASE G: μ = 0.166, α_S = 0.0° CASE I: μ = 0.3, α_S = -4.0°

Figure 3. Comparison of predicted and experimental 4P vertical hub force amplitude for 4P HHC input of amplitude θc = -0.6° as a function of phase angle.

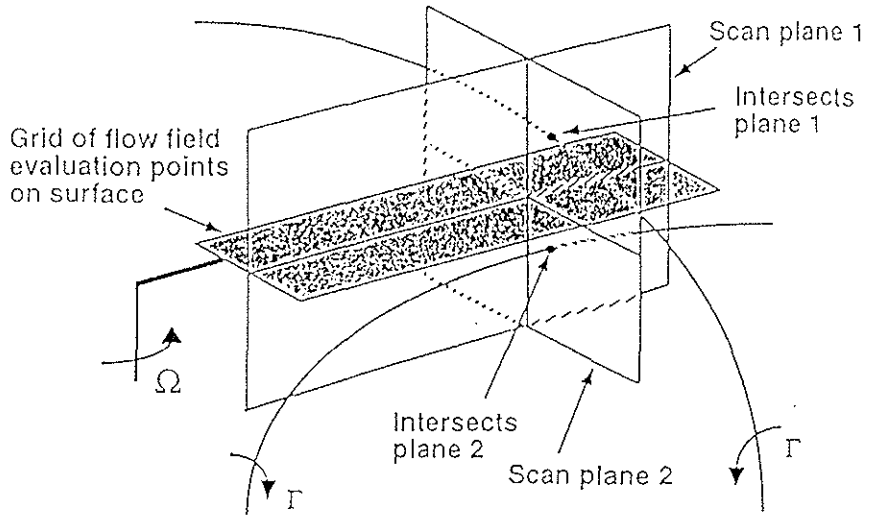

Figure 4. Typical orientation of scan planes attached to a moving blade to capture parallel and perpendicular vortex interaction events.

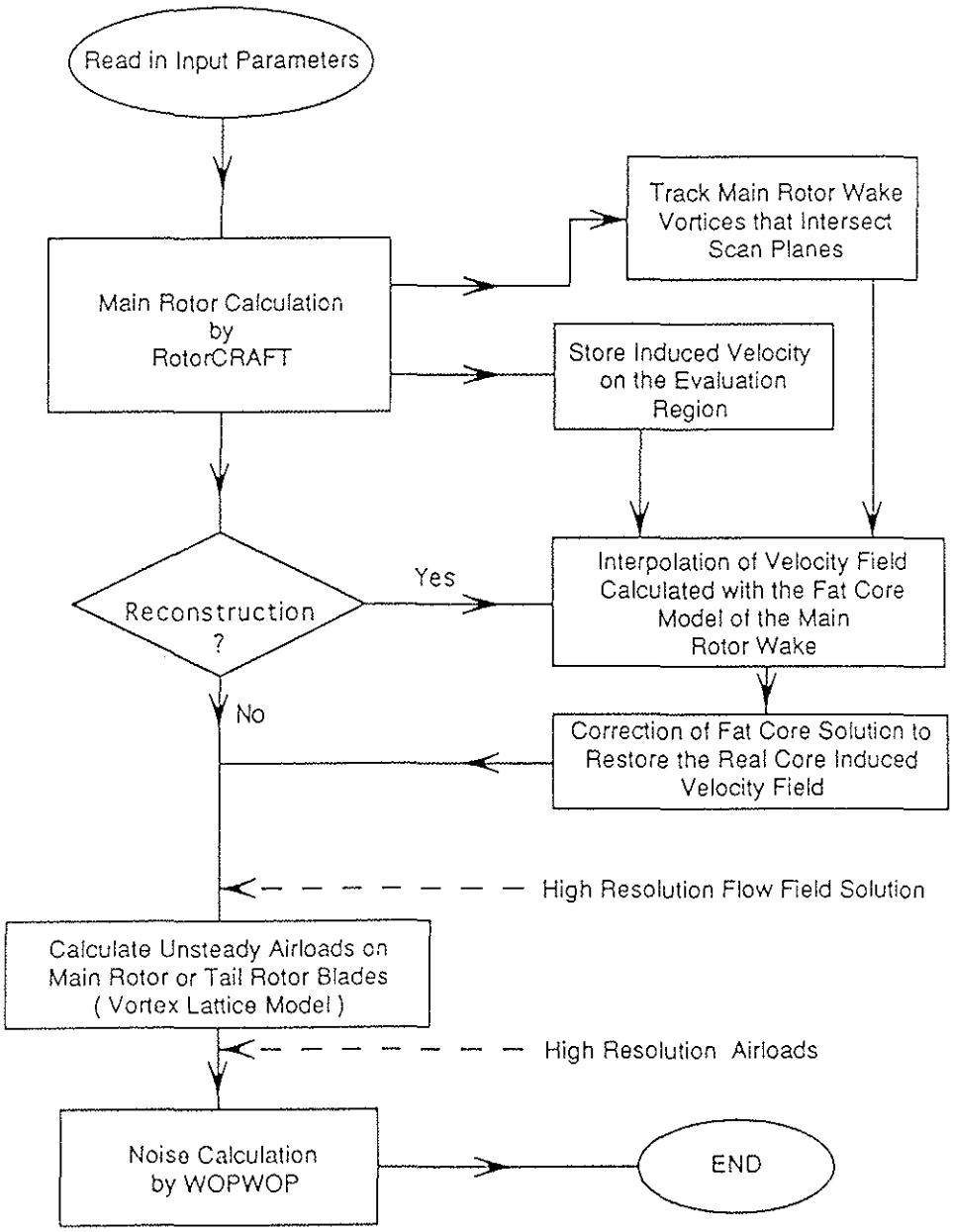

Figure 5. Simplified flow chart of program modules used for flow field and airload reconstruction.

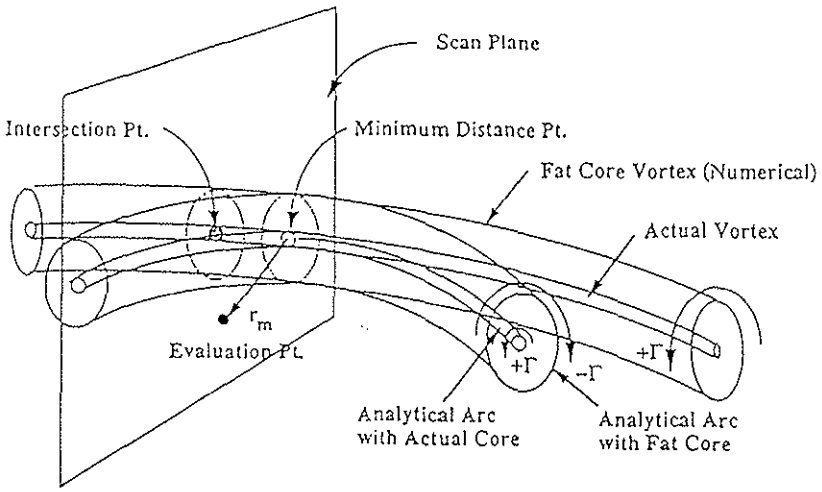

Figure 6. Schematic showing superposition of the low-resolution numerical solution and high resolution analytical solution for the nearfield velocity correction.

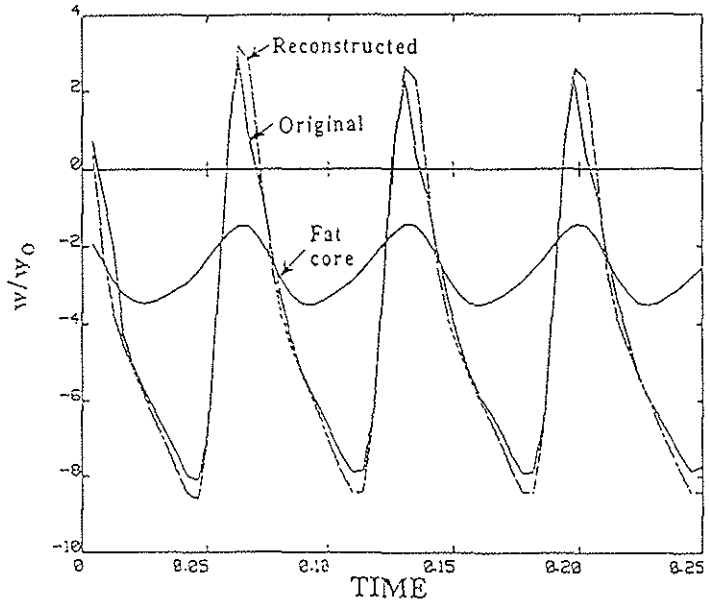

Figure 7. Comparison of actual, reconstructed and fat core downwash at a fixed point corresponding to the advancing blade tip for an H-34 at X/R = 0.0 , Y/R = 1.0 . 4:1 time interpolation used.

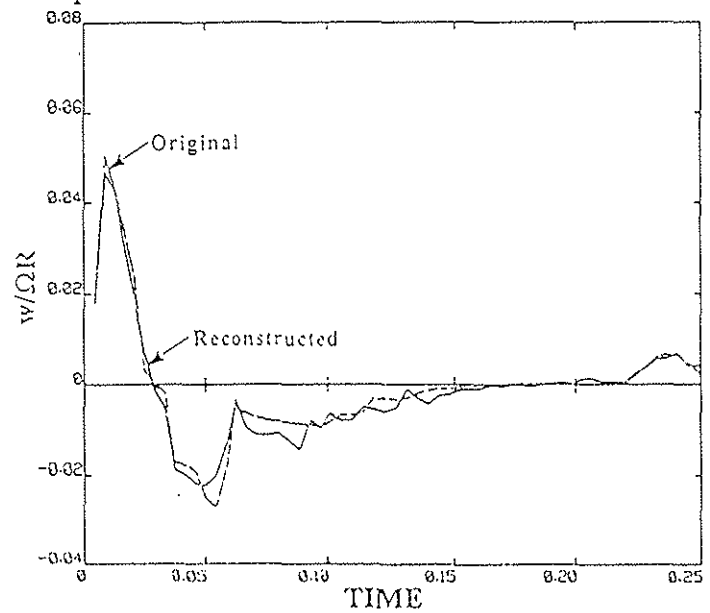

Figure 8. Original and reconstructed downwash at r/R = 0.9 on one blade of an H-34 rotor. 4:1 time interpolation used.

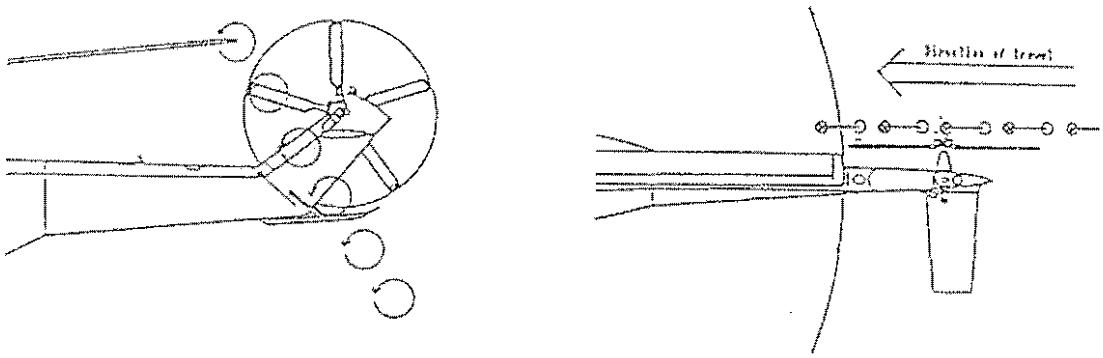

a) Schematic of main rotor/tail rotor interaction

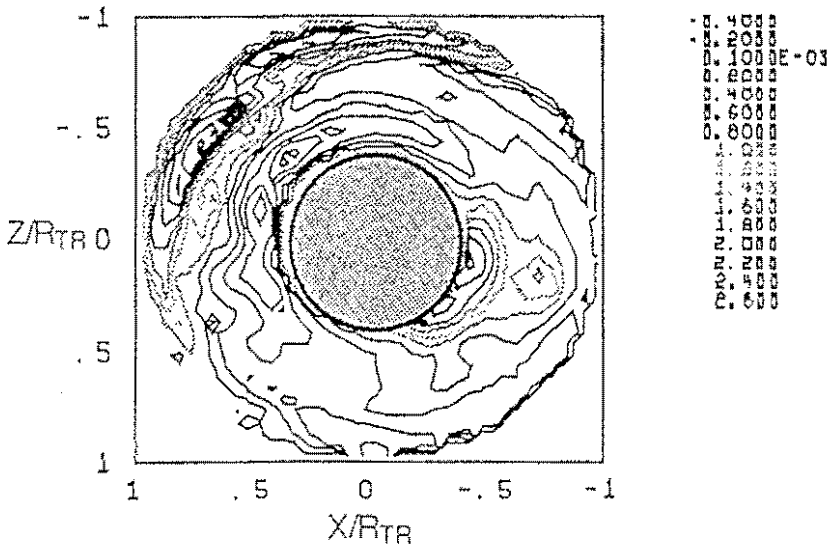

b) Plot of C_p at 2% chord

Figure 9. Azimuthal scanning polar plot of surface pressure for the instrumented blade of a Puma tail rotor at advance ratio 0.072 (Ref. 18).

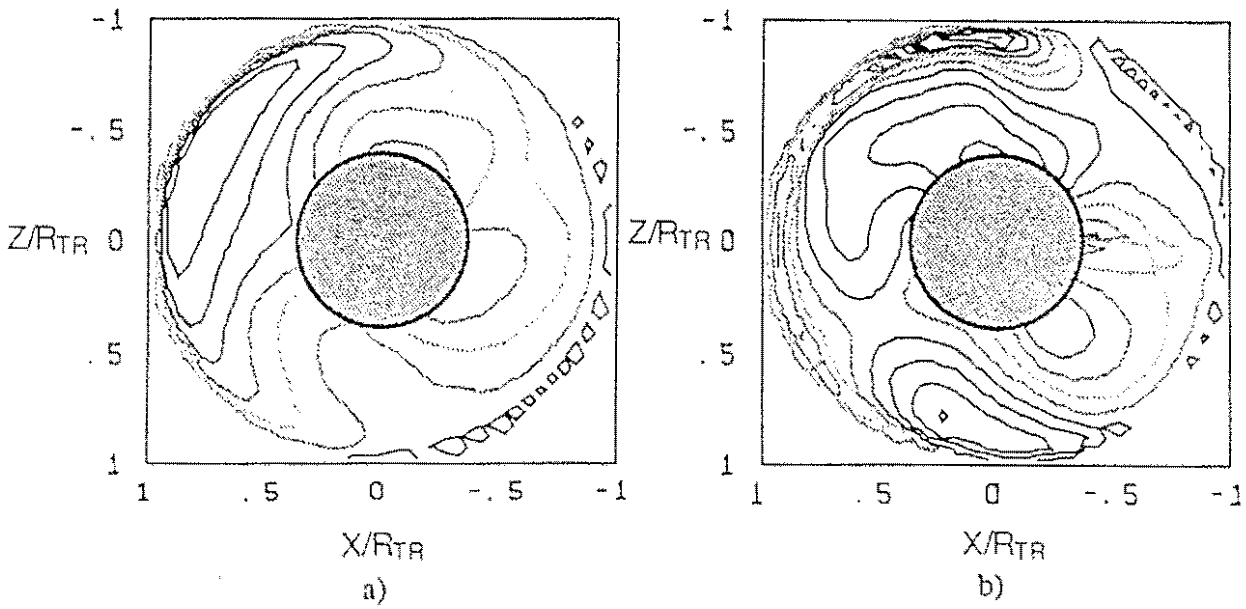

Figure 10. Prediction of surface pressure coefficient at 2% chord on the Puma tail rotor using two different models of tail rotor inflow.